Structure Characterization and Properties of Metal-Surfactant Complexes Dispersed in Organic Solvents

Pablo de la Iglesia, Vance Jaeger, Yuyin Xi, Jim Pfaendtner, Lilo D. Pozzo*

Department of Chemical Engineering, University of Washington, Seattle, Washington, USA

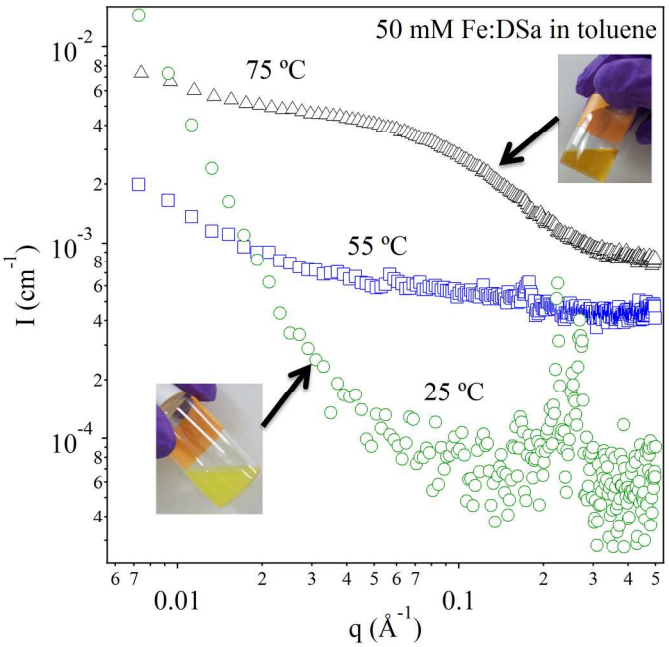

Figure S1: Fe:DSa can only be dispersed in toluene at elevated temperatures. The mixture of the salt in toluene close to room temperature has visible aggregates and it has a yellow coloration, its SAXS profile shows a rapid increase in the intensity at low-q which corroborates the presence of big aggregates. The profile also shows a series of peaks at high-q, these peaks indicate the presence of crystalline domains in the sample. As the temperature of the sample increased, there is a decrease in the slope at low-q and the peaks at high-q start to disappear. At 75 ºC the crystalline peaks disappear and the low-q behavior is similar to other iron complexes. The appearance of the mixture also changes, going from a cloudy yellow mixture to orange and clear (without visible aggregates).

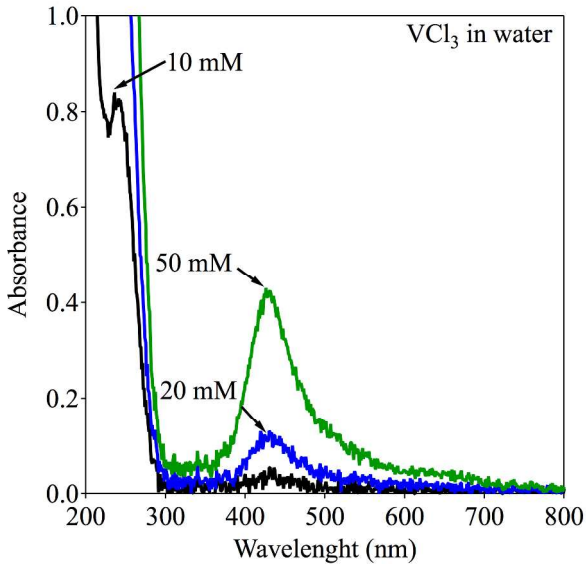

Figure S2: UV-vis spectroscopy of VCl_3 aqueous solution at different concentrations is performed using a Thermo Scientific Evolution 300 (Fremont, CA) spectrophotometer covering wavelengths from 200 to 800 nm. A quartz cuvette with a 1 mm path length is used in order to keep the absorbance within the instrumental range. The peak at ~400 nm is characteristic of V(V) oxidation, furthermore the lack of peaks at 600, 800 and 850 indicates the absence of the other oxidation states of vanadium.[1]

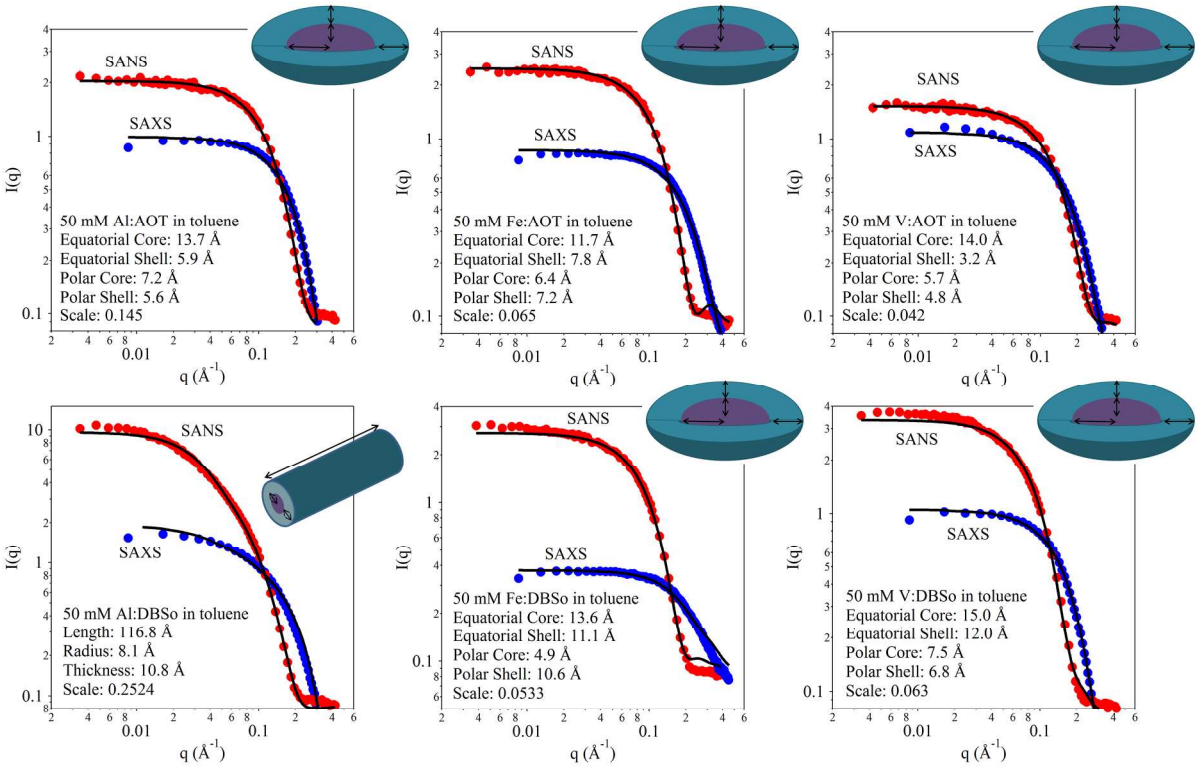

Figure S3: SANS and SAXS scattering profiles of the different organometallic salts used in this study, dispersed in toluene. The black lines are the simultaneous fits obtained using the core-shell ellipsoid or cylinder form factors. The parameters from the fits are found in Table 1 in the main manuscript.

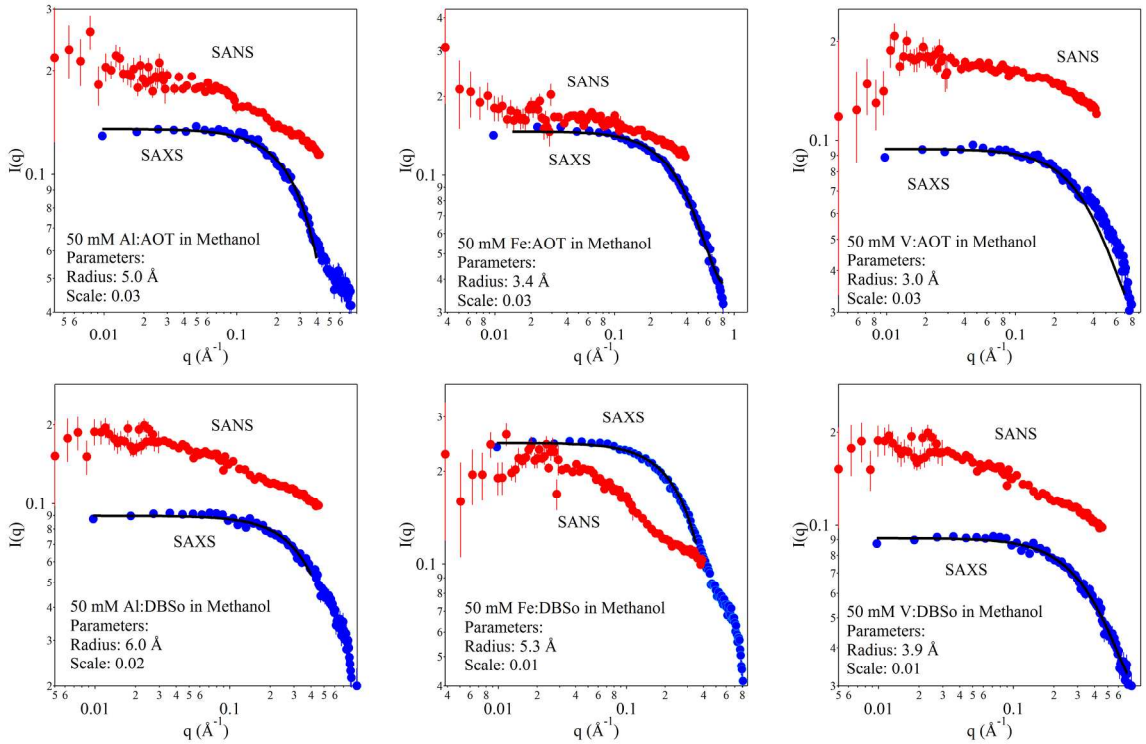

Figure S4: SANS and SAXS scattering profiles of different organometallic salts dispersed in methanol. The black lines are best fits to form spherical factors. The parameters from the fits are shown in Table 2 in the main manuscript.

Table S1: Number of molecules of each type in the simulation boxes. After pressure equilibration, cubic box side length ranges from 6.8 to 7.8 nm depending on the system. Density fluctuations are small after equilibration.

	Number of molecules			
Molecule	**DBSo-Methanol**	**DBSo-Toluene**	**AOT-Methanol**	**AOT-Toluene**
DBSo	24	24	-	-
AOT	-	-	24	24
Fe^{3+}	8	8	8	8
Methanol	4470	-	4470	-
Toluene	-	2448	-	2448

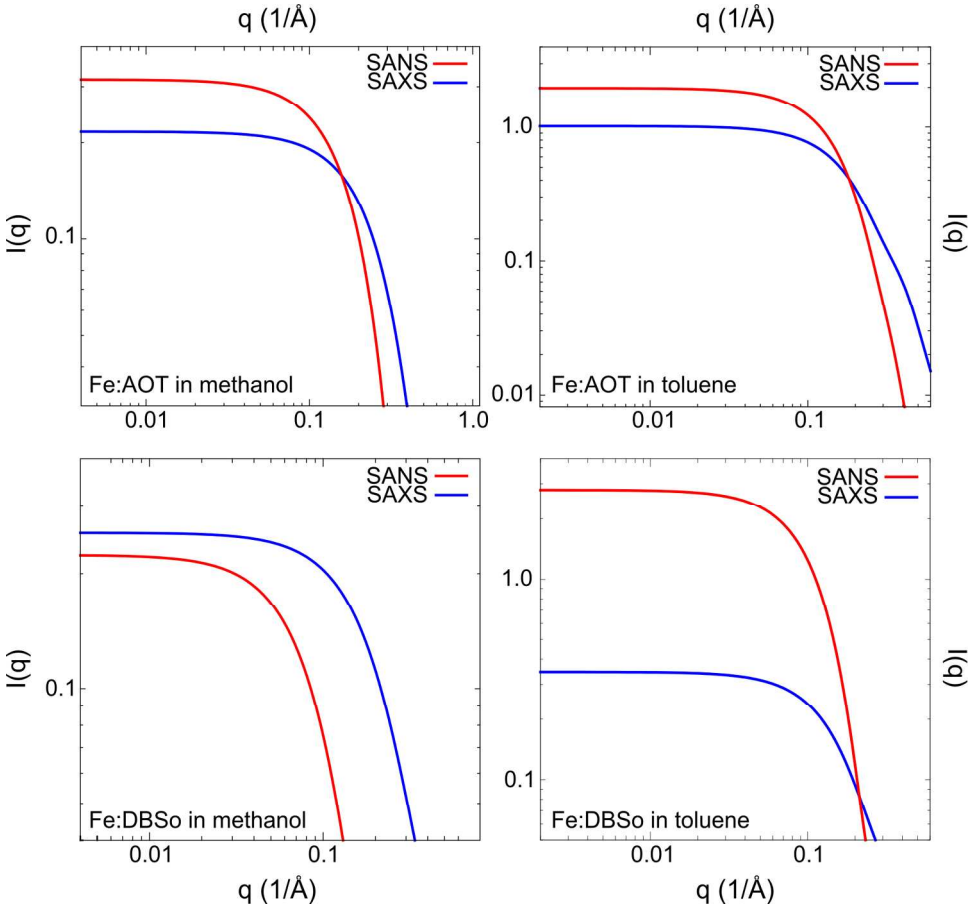

Figure S5: Scattering curves of dominant structures from simulations.

Curves are calculated using Crysol and Cryson.[2,3] Dominant structures were extracted from the simulations. Ten frames of data are averaged for each curve. Locations of the major features can be compared to the experimental data.

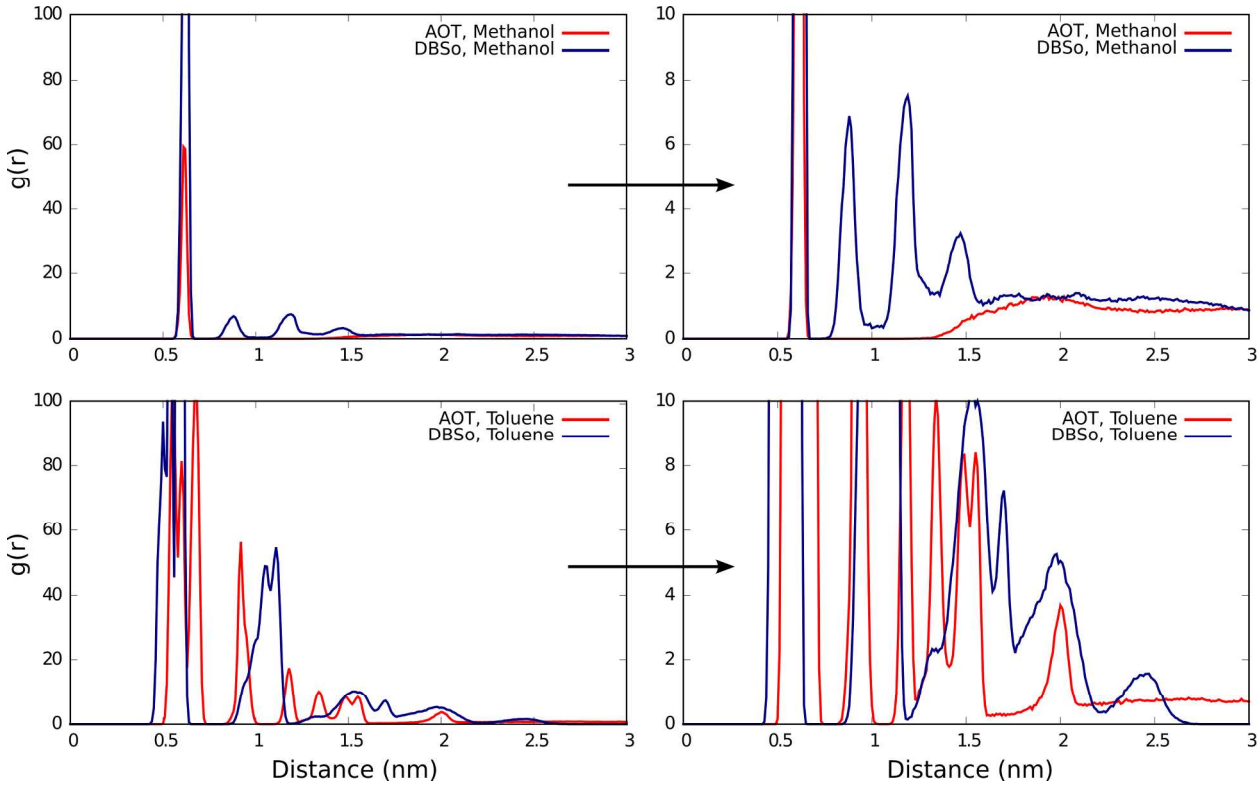

Figure S6: Radial distribution functions for iron ions in simulated complexes

The radial distribution function illustrates the structuring of the iron ions in the simulations. The left panel shows a wide range for the y-axis while the right panel zooms the y-axis to accentuate the detail of the hills at high distances. Those complexes solvated in toluene have structure over much larger distances. Moreover, we can see that the structuring of these toluene-solvated complexes extends over distances of up to 2.5 nm. DBSo in toluene has longer-range structuring than AOT in toluene. The distances and the trends are consistent with the equatorial core radii (notice radii rather than diameters) obtained from SAXS. The methanol simulations show much less or no long-distance structuring. AOT in methanol has a peak around 0.6 nm, which corresponds to a complex with two irons at the core. Only two such complexes are observed, and all other complexes in the simulations contain one iron ion. DBSo in methanol is more complicated. There are interactions between the chains of neighboring complexes, and this causes some iron cores to be close to each other while not being in the same complex-core. The radial distribution function corresponds to an average core size that is larger than the one observed for AOT in methanol. This is consistent with the SAXS data.

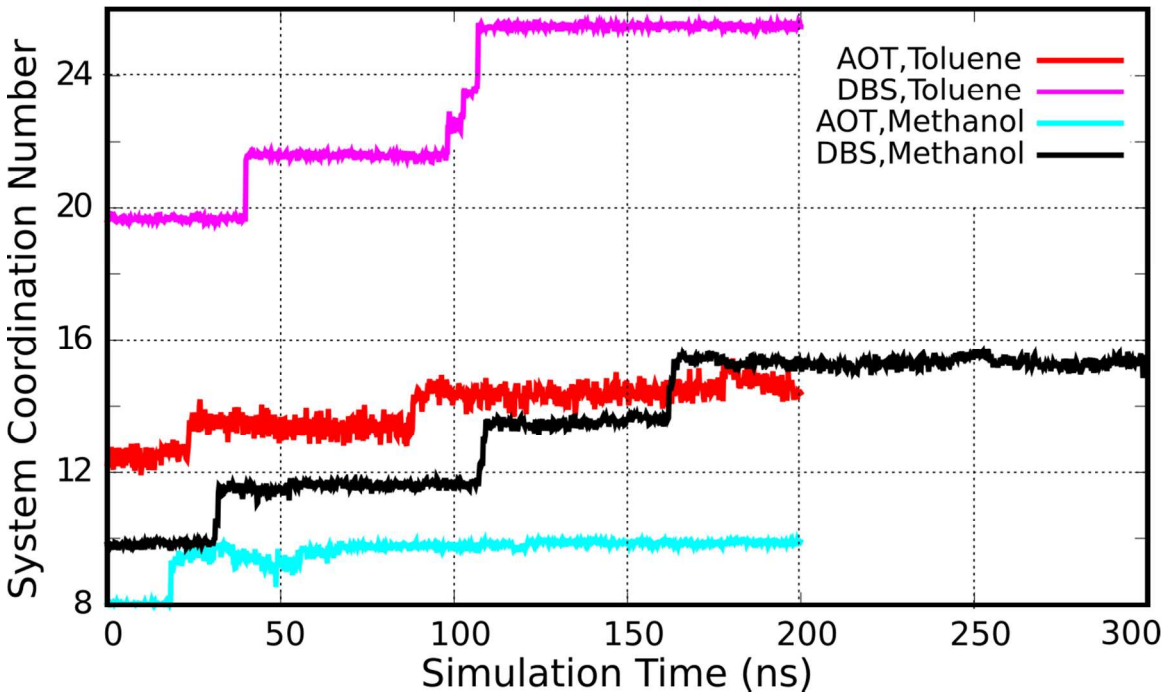

Figure S7: The coordination number for each of the systems over the length of the production trajectory.

Convergence of the simulations was measured by calculating the coordination of the iron atoms in the system. The coordination (s) of any pair of irons is given by a sigmoidal function that decays smoothly from one to zero as the distance (r) between the ions increases. The sigmoidal function takes the following form, where the $r_0 = 0.7$ nm, $n = 20$, and $m = 40$.

$$s = \frac{1-(r/r_0)^n}{1-(r/r_0)^m} = \frac{1=(r/0.7)^{20}}{1-(r/0,7)^{40}} \qquad \text{Equation S1}$$

The system coordination number is the sum of s over all pairs of iron ions in the system. A value of 8 represents a system that has no coordinating ions, and only the self-interaction is counted. Higher values correspond more and/or larger clusters of iron ions.

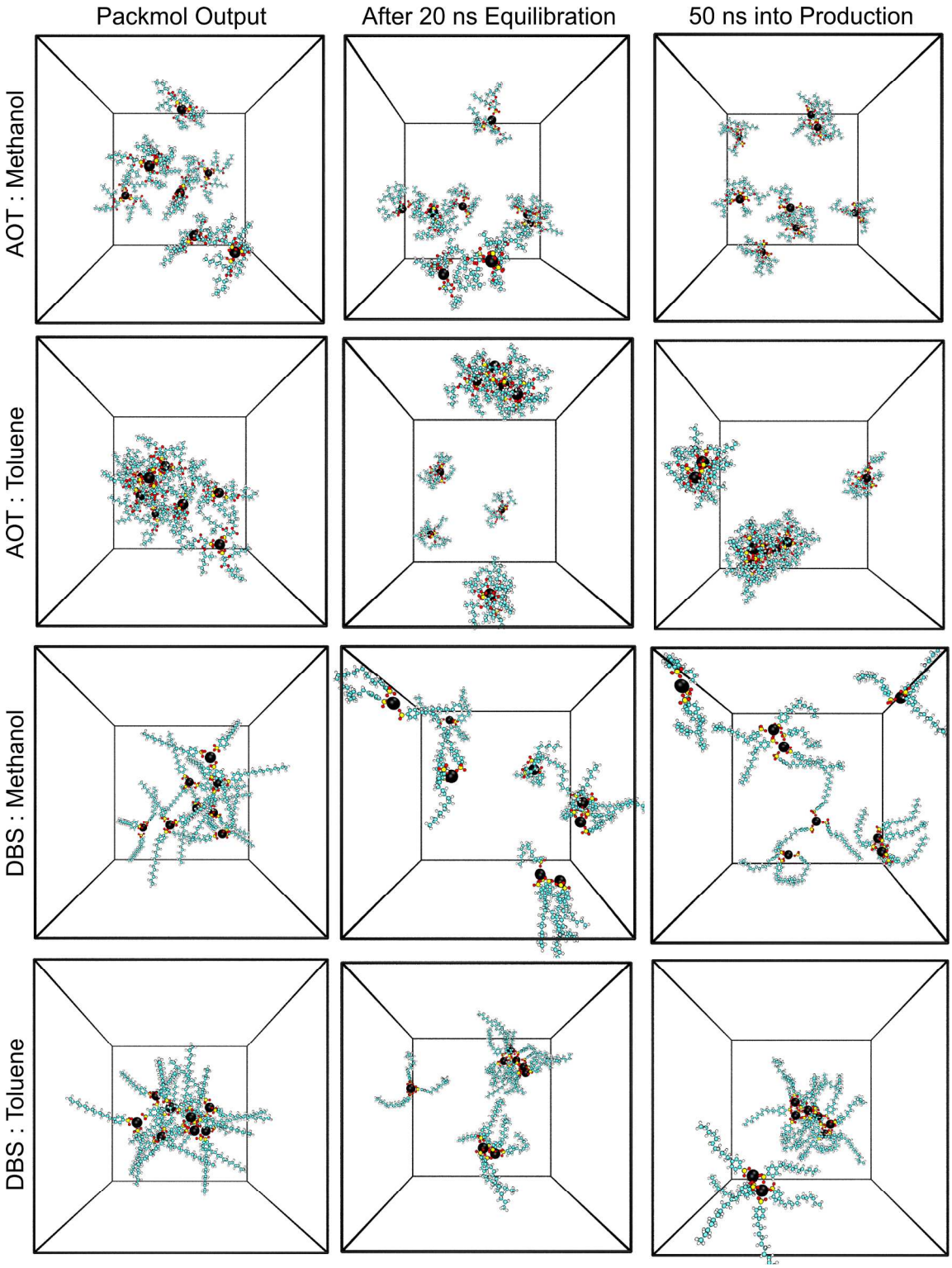

Figure S8: Snapshots of the formation of the complexes during the simulations.

Snapshots of the simulations are displayed. Packmol was used to pack the simulation boxes. Production simulations are preceded by 20 ns of pressure equilibration (Berendsen barostat).

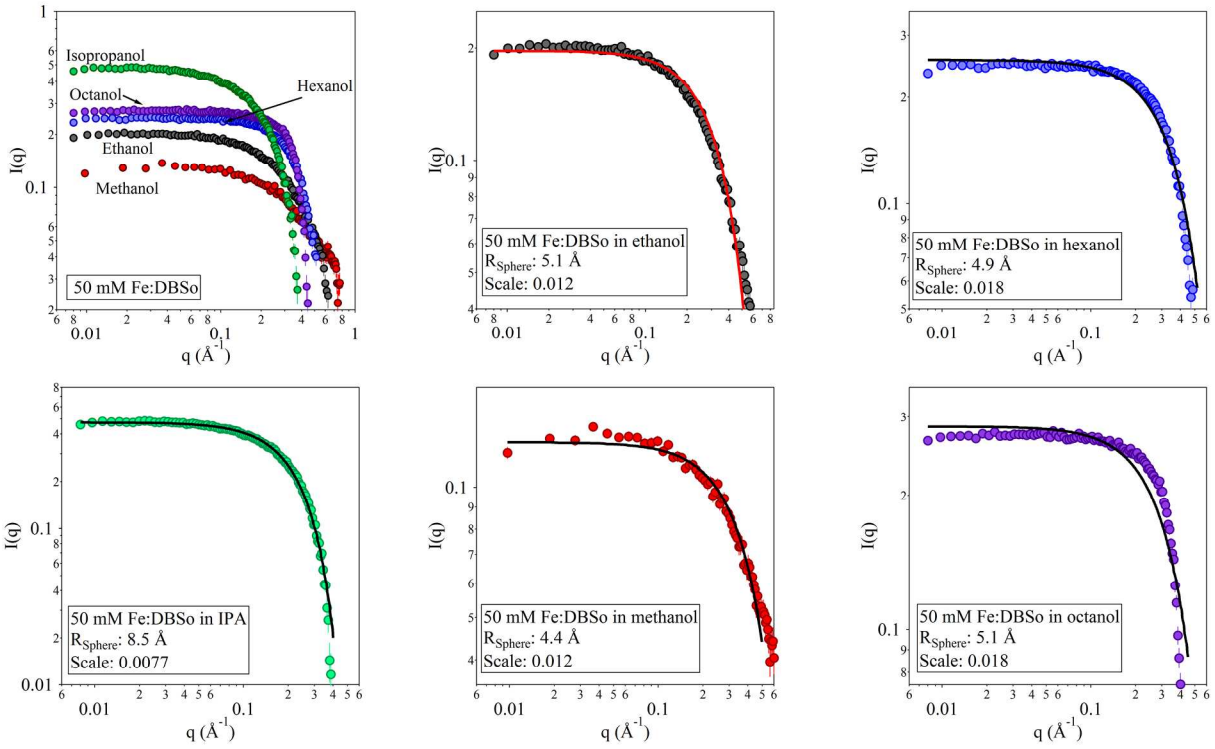

Figure S9: SAXS patterns for Fe:DBSo in several different alcohols. The Guinier region for all SAXS profiles changes very little for a wide range of alcohols. The isopropanol sample shows a larger change. For most the fit reveals similar dimensions (4-5 Å in radius) and similar scale factor. The difference in the intensity of the scattering profiles is caused by a changing contrast from the scattering length densities of the different alcohols.

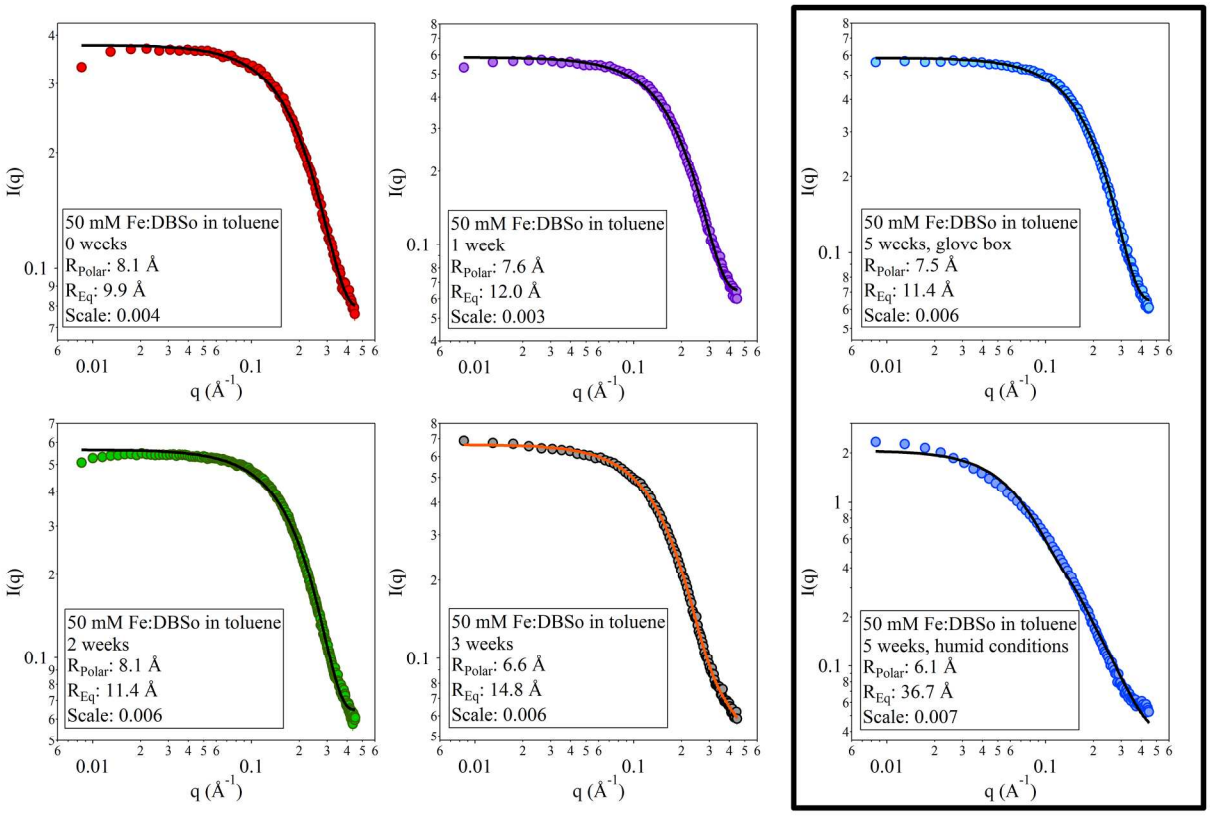

Figure S10: SAXS profiles showing the aging of Fe:DBSo in toluene. An ellipsoid model is used to fit all profiles. The scattering describe the core of the metal complex, and indicates swelling and growth of the micellar domains in the sample. The profiles inside the rectangle are obtained after 5 weeks under inert (top) and humid (bottom) conditions. The sample under inert conditions show similar characteristics to the 1-week old sample aged at room conditions, Meanwhile the sample under humid conditions evolves into a cylinder far longer than the original samples.

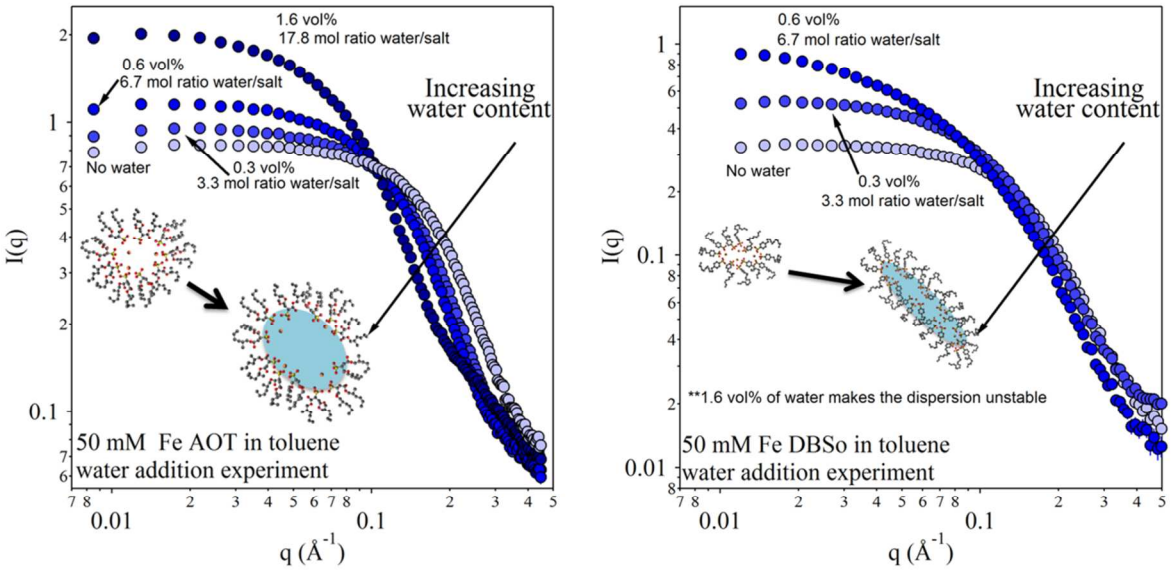

Figure S11: SAXS profiles demonstrating the effect of water in the structural conformation of the organometallic complexes dispersed in toluene.

Water is added to the organometallic complex prior to the addition of the solvent in order to ensure the water-complex interaction is not hindered by the hydrophobicity of the solvent. The Fe:AOT microemulsion swell with the addition of water, this phenomenon has been studied previously.[4-6] The evolution of the Fe:AOT with added water seems to differ from the aging Fe:AOT dispersion (figure 6 in the main manuscript). In figure 6 the scattering indicates an aggregation of the micellar domains. The changes depicted in figure S11 show an increase in the size of the micelle but no indication of aggregation. The scattering of Fe:DBSo changes into a similar profile to the one observed under humid conditions (figure S10), which seems to indicate that the addition of water and aging in the sample causes the micelle to evolve in similar way.

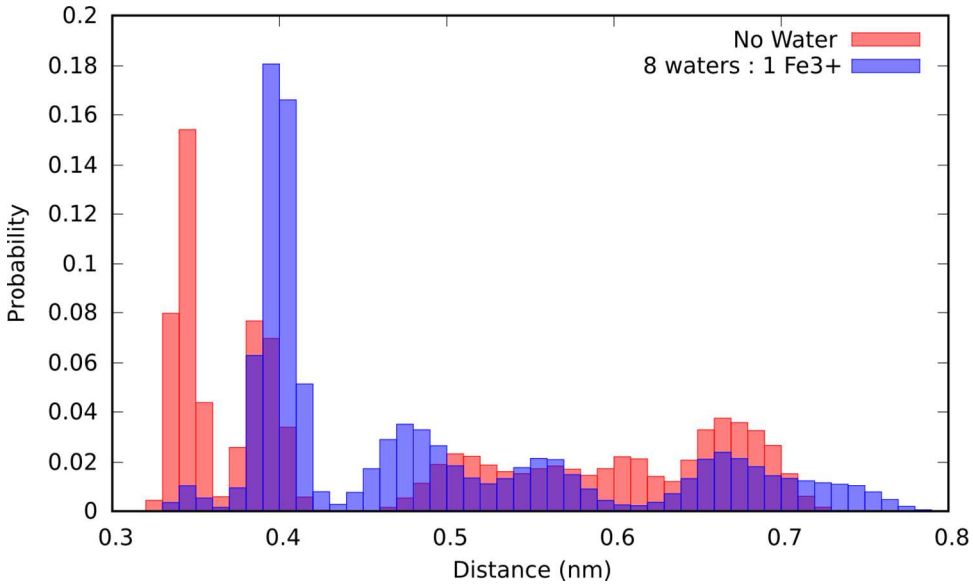

Figure S12: Probability distribution of interatomic distances for sulfur and iron atoms in a simulations of Fe^{3+}:AOT in toluene

In order to gain insight into the effects of water on the structure of the complexes, a 100 ns simulation of the AOT in toluene system was run using the same protocol as described in the methods section of the main text. Sixty-four TIP3P water molecules were added. The interatomic distances of all sulfur and iron atoms were calculated. The histogram of these distances shows that the presence of water causes the core to swell. All of the peaks are broadened and shifted to higher distances. This is because the water molecules penetrate the core and intercalate themselves between the iron ions and the nearby sulfurs. This explains the swelling observed in Figure S11.

We also examined the question of whether trace monovalent ions, such as sodium or chlorine that could be introduced with the organic salt, might affect the formation of the complexes in organic solvents. We note that any residual ions that could perhaps be introduced would be at very low concentrations since their presence cannot be detected in XPS experiments. Nevertheless, to evaluate their possible effect, an additional 100 ns simulation was conducted with 8 Na^+ ions and 8 Cl^- ions in the AOT toluene system. Note that this would represent a very large concentration since only 8 Fe^{+3} ions are simulated in each system. The final structures of the complexes were very similar for the ion-free and ion-containing simulations. The ion-free simulation contained three complexes with five, two and one iron respectively. The ion-containing simulation contained three complexes with six, one, and one iron respectively. Four sodium and four chloride ions were incorporated into the complexes.

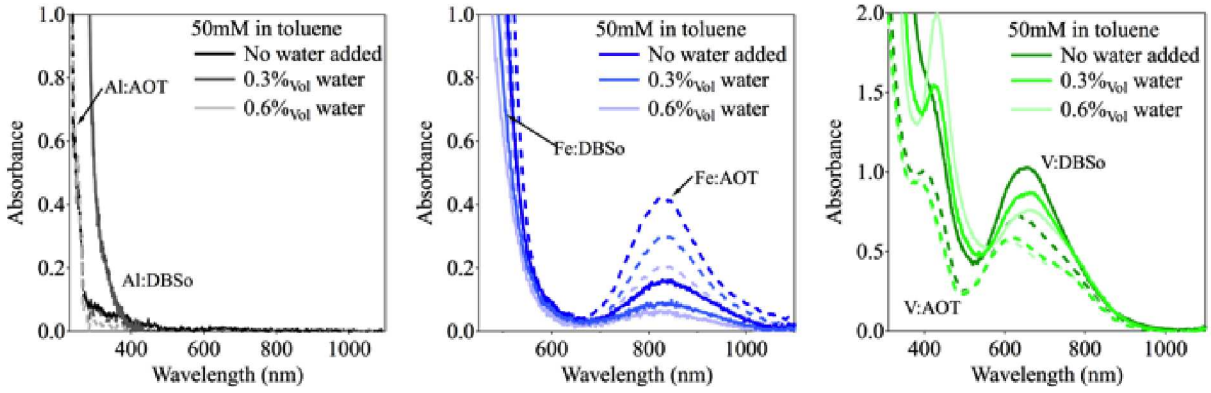

Figure S13: UV-vis spectroscopy of organometallic complex dispersed in toluene (50 mM) is performed using a Thermo Scientific Evolution 300 (Fremont, CA) spectrophotometer covering wavelengths from 200 to 800 nm. A quartz cuvette with a 1 mm path length is used in order to keep the absorbance within the instrumental range. UV-vis absorbance of metallic complexes in toluene with different levels of hydration. AOT complex are shown in dashed lines and DBSo in solid lines. Aluminum complexes show no absorbance in this wavelength range. Iron complexes show a single peak at around 820 nm and the intensity decreases as the water content increased. Vanadium complexes show two absorbance peaks at 400, 600 nm and a shoulder at ~700 nm. All peaks decrease in intensity as water is added. The peak at 400 is related to a V(V) oxidation state, while a peak at 600 is for V(III),and the shoulder at ~700 could represent the presence of V(IV).[1] Ultimately this shows that, after the formation of the vanadium complexes, there are several redox states present in the samples.

References

1. Choi, N. H.; Kwon, S.-K.; Kim, H., Analysis of the Oxidation of the V(II) by Dissolved Oxygen Using UV-Visible Spectrophotometry in a Vanadium Redox Flow Battery. *J. Electrochem. Soc.* **2013**, *160*, (6), A973-A979.
2. Svergun, D.I., Barberato, C., Koch, M.H.J., CRYSOL- A Program to Evaluate X-Ray Solution Scattering of Biologial Macromolecules for Atomic Coordinates. *J. Appl. Cryst.* **1995,** *28*, 768-773.
3. Svergun, D.I., Richard, S., Koch, M.H.J., Sayers, Z., Kuprin, S., Zaccai. Protein Hydration in Solution: Experimental Observation by X-Ray and Neutron Scattering. *Proc. Natl. Acad. Sci.* **1998,** *95*, 768-773.S.
4. Eastoe, J.; Towey, T. F.; Robinson, B. H.; Williams, J.; Heenan, R. K., Structures of Metal Bis(2-Ethylhexyl) Sulfosuccinate Aggregates in Cyclohexane. *J. Phys. Chem.* **1993**, *97*, (7), 1459-1463.
5. Morrison, I. D., Electrical Charges in Nonaqueous Media. *Colloid Surface A.* **1993**, *71*, (1), 1-37.

6. Eastoe, J.; Fragneto, G.; Robinson, B. H.; Towey, T. F.; Heenan, R. K.; Leng, F. J., Variation of Surfactant Counterion and its Effect on the Structure and Properties of Aerosol-OT-Based Water-in-Oil Microemulsions. *J. Chem. Soc. Faraday T.* **1992**, *88*, (3), 461-471.